A New Tetra-Zr(IV) Substituted Polyoxotungstate Aggregate

Hai-Lou Li, Yue-Lin Wang, Zhong Zhang, Bai-Feng Yang, and Guo-Yu Yang*

MOE Key Laboratory of Cluster Science, School of Chemistry and Chemical Engineering, Beijing Institute of Technology, Beijing 102488, China. E-mail: ygy@bit.edu.cn

Electronic Supplementary Information

The refinement details in 1

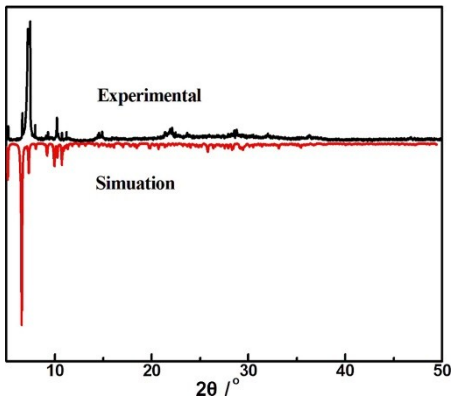

Figure S1. The experimental and simulated PXRD patterns of **1**.

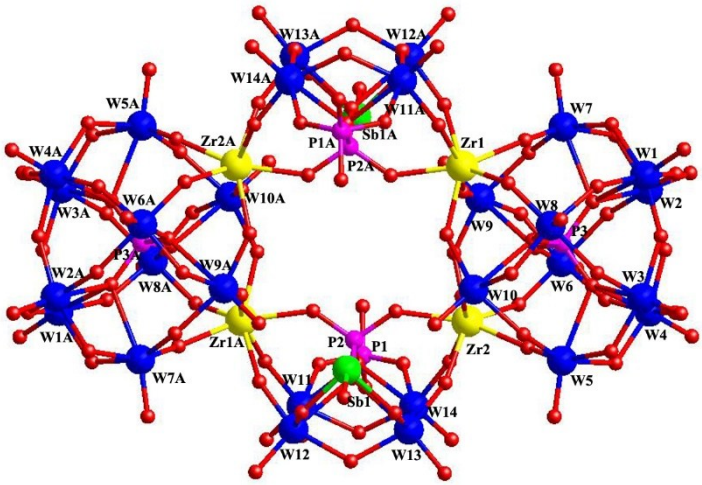

Figure S2. The polyoxoanionic structure of the **1**. W (blue balls), Zr (brilliant yellow balls), O (red balls), P (pink balls) and Sb (brilliant green balls). Atoms with A in their labels are symmetrically generated. A: 1–*x*, 2–*y*, 1–*z*.

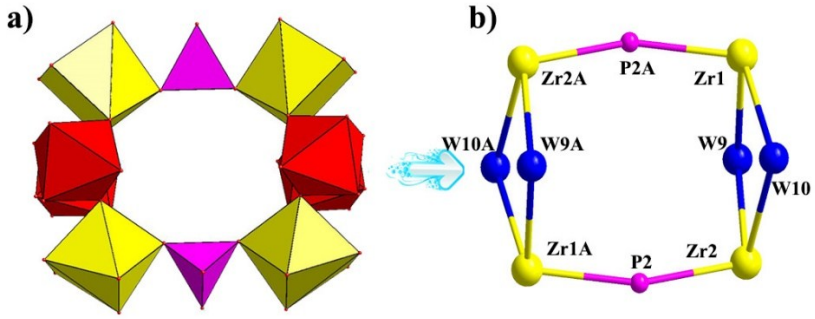

Figure S3. (a) The polyhedral view of ring the $\{Zr_4W_4P_2\}$; (b) The simplified packing of $\{Zr_4W_4P_2\}$.

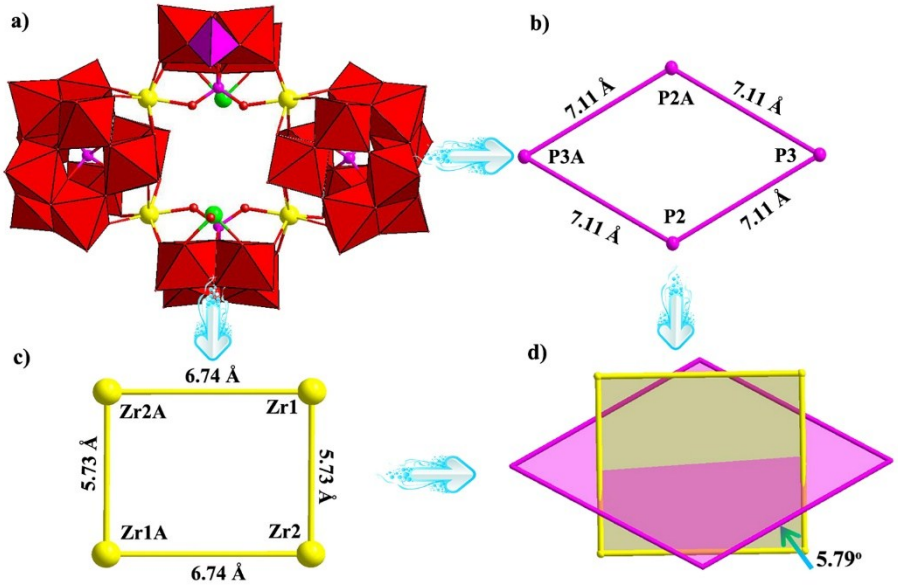

Figure S4. (a) The structure of **1a**; (b) The lozenge of the four P atoms (P2, P3, P2A and P3A); (c) The rectangle of the four Zr^{4+} ions ($Zr1^{4+}$, $Zr2^{4+}$, $Zr1A^{4+}$ and $Zr2A^{4+}$); (d) The angle between lozenge and the rectangle.

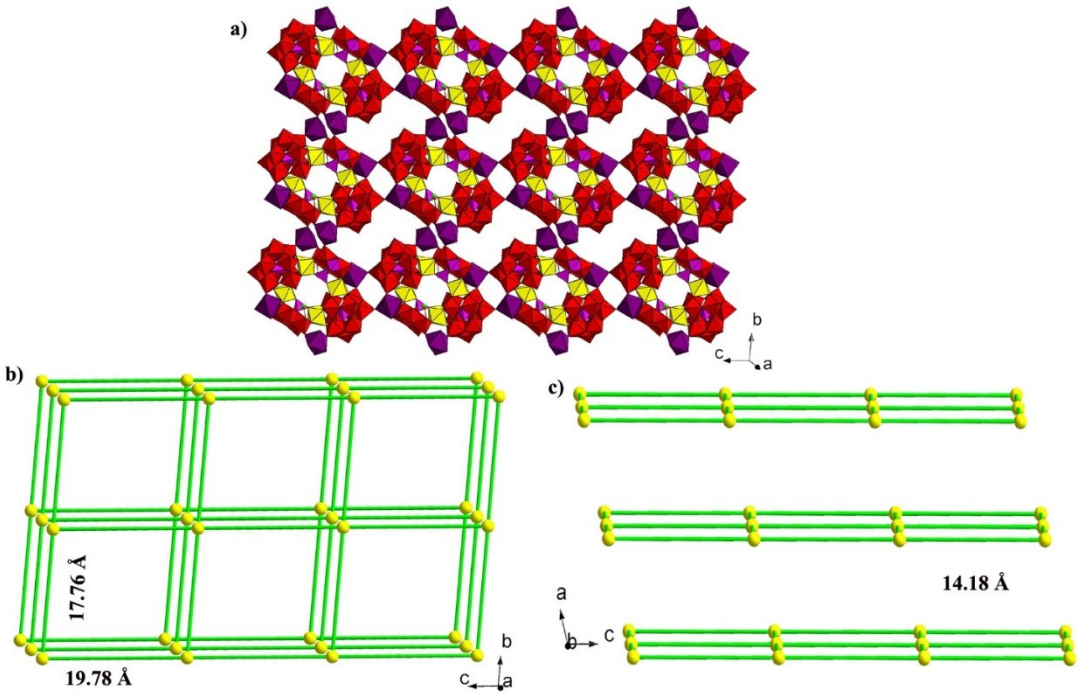

Figure S5. (a) The view of the extraordinary 2-D pillar-supporting architecture along the *a* axis in **1**. Lattice water molecules, $[H_2N(CH_3)_2]^+$ and no acting as a bridged Na^+ ions are omitted for clarity. (b) The simplified packing of **1** viewed along the *a* axis. (c) The simplified packing of **1** viewed along the *b* axis.

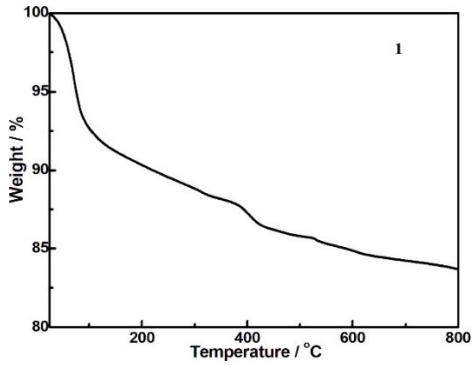

Figure S6. The TG curve of **1**.

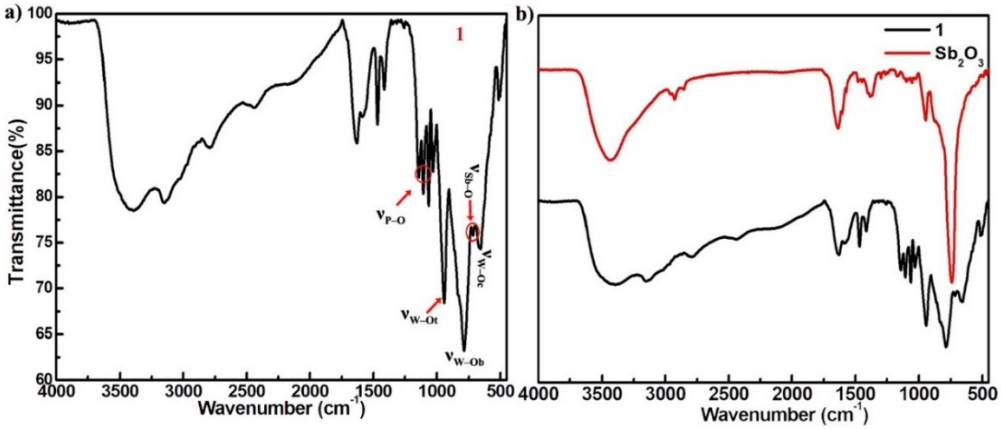

Figure S7. (a) The IR spectrum of **1**. (b) The IR spectra of **1** and Sb_2O_3.

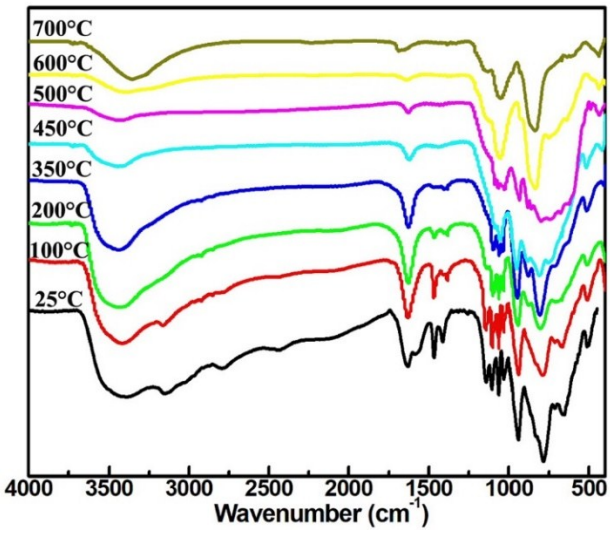

Figure S8. The IR spectra of **1** at different temperatures.

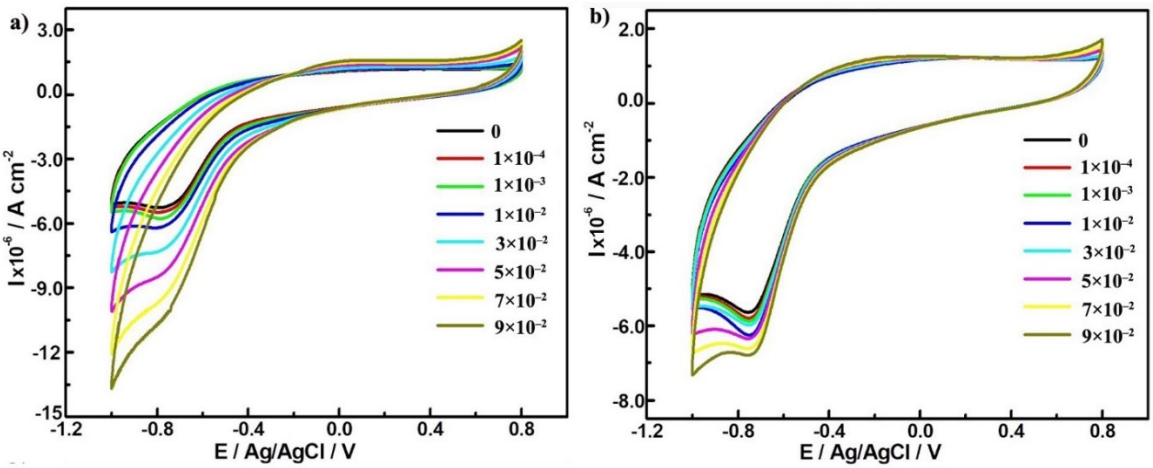

Figure S9. (a) The cyclic voltammograms of **1** at various concentrations of H_2O_2. (b) The cyclic voltammograms of **1** at the different concentrations of $NaBrO_3$.

Table S1. Bond valence sum (BVS) calculations of all W, Zr, Sb, P and O atoms in **1a**.

Atom	BVS	Atom	BVS	Atom	BVS
W1	6.178	W2	6.167	W3	6.122
W4	6.323	W5	6.320	W6	6.150
W7	6.183	W8	6.170	W9	6.300
W10	6.142	W11	6.310	W12	6.096
W13	6.280	W14	6.177		
Zr1	3.900	Zr2	3.883		
Sb1	2.790				

P1	5.121	P2	5.110	P3	5.055
O1	1.390	O2	1.478	O3	1.862
O4	2.015	O5	2.009	O6	1.919
O7	1.829	O8	1.855	O9	1.870
O10	1.978	O11	1.909	O12	1.903
O13	1.998	O14	1.922	O15	1.877
O16	1.974	O17	2.058	O18	1.989
O19	2.060	O20	1.758	O21	1.860
O22	1.916	O23	2.291	O24	1.870
O25	1.867	O26	2.011	O27	1.968
O28	1.698	O29	0.994	O30	1.764
O31	1.712	O32	1.931	O33	1.712
O34	1.680	O35	1.716	O36	1.740
O37	1.778	O38	1.680	O39	1.676
O40	1.977	O41	1.717	O42	1.934
O43	1.640	O44	2.025	O45	1.928
O46	1.998	O47	2.050	O48	1.877
O49	1.745	O50	1.676	O51	1.877
O52	1.891	O53	2.027	O54	1.826
O55	1.895	O56	1.985	O57	1.922
O58	1.939	O59	1.834	O60	2.016
O61	1.870				

Table S2. The peak potentials for all the redox waves for **1** determined by CV in 0.5 mol·L^{-1} Na_2SO_4 + H_2SO_4 aqueous solution at pH = 5.6. Scan rate: 50 mV·s^{-1}.

I / V	**I′ / V**	**$E_{1/2}$ / V**	**ΔE_p / V**
–0.712	–0.502	–0.607	–0.210
II	**II′**		
–0.304	–0.160	–0.232	–0.144

Table S3. The CAT versus concentration of H_2O_2 and $NaBrO_3$ for **1**.

C / mol L^{-1}	1×10^{-4}	1×10^{-3}	1×10^{-2}	3×10^{-2}	5×10^{-2}	7×10^{-2}	9×10^{-2}
CAT (H_2O_2)	4.22%	9.98%	19.19%	39.92%	64.49%	90.40%	109.40%
CAT (Na_3BrO_3)	5.48%	7.31%	9.32%	14.62%	16.45%	21.21%	25.59%